

IOT Based Data Logger For Surveil And Detection Of Laneline Crossing System

N. Priyadharshini¹, M. Bhuvaneshwari², M. Narmatha³, Mr. A. Poomaran⁴

^{1, 2, 3}Dept of Electronics and Communication Engineering

⁴HOD, Dept of Electronics and Communication Engineering

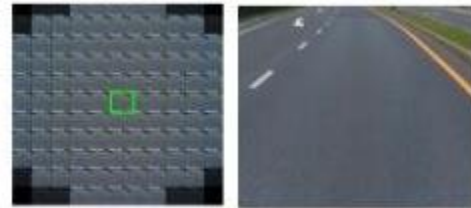
^{1, 2, 3, 4}NSN college of Engineering and Technology, Karur, Tamilnadu, India,

Abstract- Robust lane detection is imperative for the realization of intelligent transportation. Recently vision based systems that employ deep convolution networks (CNNs) for lane detection have made for considerable progress. However, for better generalization under various road condition learning based methods required excessive training data, which become non trivial in challenging conditions such as illumination variation, shadows, false lane line detection and worn lane markings. In this paper, we propose a light field(LF) based lane detection method that utilize additional angular information for improved for prediction and increased robustness. IoT based smart transport systems are receiving huge attention among public. Vehicles implanted with huge number of sensors permit the people to monitor present state of the vehicle. The accident information system will alert vehicle owner or relative, nearby hospital through GSM module with location by GPS. All the information recorded by vehicle black box for future investigation.

Keywords- laneline detection, deep learning(CNN), accident monitor, sensors, GSM, GPS.

I. INTRODUCTION

One of the major contributing factors of road traffic accidents (RTAs) can be attributed to human error, which can be caused by several factors, including but not limited to distractions, fatigue, and misbehavior. Recently, traffic on roads has been increasing rapidly a result of which it is becoming extremely difficult to manage vehicles in terms of traffic management, vehicle theft, and accidents. United States is stolen estimating a loss of over \$9 billion per annum. Several tools and techniques are used to minimize the probability of such incidents while preserving the safety of the people involved. Vehicle tracking is an old concept and has been implemented across the globe for tracking stolen vehicles or sometimes for personal safety. Several methods have been proposed and implemented worldwide to overcome these issues. How ever the cost of these solutions varies and is dependent on technology used. The most common tool used today is Global Positioning System (GPS), which is discussed further in this paper.



A decoded light field using Matlab's light field toolbox [16], along with a middle perspective image.

II. LITERATURE SURVEY

1. CLRNet: Cross Layer Refinement Network for Lane detection: Lan detection using MATLAB with light field tool.
2. A Dynamic Bayesian Network Model for Real Time Risk propagation of secondary Rear End Collision Accident Using Driving Risk Field: Secondary rear end collision ,risk propagation, driving risk field, dynamic Bayesian.
3. Smart Characterization of Vehicle Impact and Accident Reporting System: To detect the impact and identify if it is an accident or a minor collision using sensors.
4. Modeling of a Road Traffic Accident Using Multivariate Analysis of Injuries in a Two-Wheeled Vehicle Collision with a Car: In this study is to study the kinematics of the road accidents movement and the factors influencing the degree of injury from collisions of a two- wheeled vehicle with a car by modeling a road traffic accident.
5. DeepCrash: A Deep Learning-Based Internet of Vehicles System for Head-On and Single-Vehicle Accident Detection with Emergency Notification: This paper a deep learning-based Internet of Vehicles (IoV) system called Deep Crash, which includes an in-vehicle infotainment (IVI) telematics platform with a vehicle self-collision detection.
6. An IoT Based Automatic Accident Detection and Tracking System for Emergency Services: The proposed research work aims to work on this topic by building an automated system to alert the family member as soon as the occurrence of the accident.
7. Categorized Accident Alerting System Using Bike Gloves: Accidents can be detected and informed to the

authorized person and rescue team according to the category of the accident.

- Accident Alert system application using a privacy preservation block chain-based incentive mechanism: This paper provides an innovative solution by developing an Accident Alert Message System using an Android Smartphone Application that can be used from the accident zone.

III. EXISTING METHOD

Lane is critical in the vision navigation system of the intelligent vehicle. This paper presents Cross layer refinement network aiming at fully utilizing both high level and low level features in lane detection using MATLAB with light field tool. CLNet can exploit high level features to predict lanes while leverage local detailed features to improve localization accuracy. ROIgather to enhance the representation of lane features by building relations with all pixels. IoU loss tailored for lane detection, which considerably improve performance compared with standard loss and smooth loss.

DRAWBACK:

- Light fields require capturing and processing multiple images from different viewpoints.
- time-consuming.
- The processing and analysis of the data is complex than traditional image processing techniques.
- Increased overall processing time and decrease the real-time performance of the system.

IV. PROPOSED METHOD

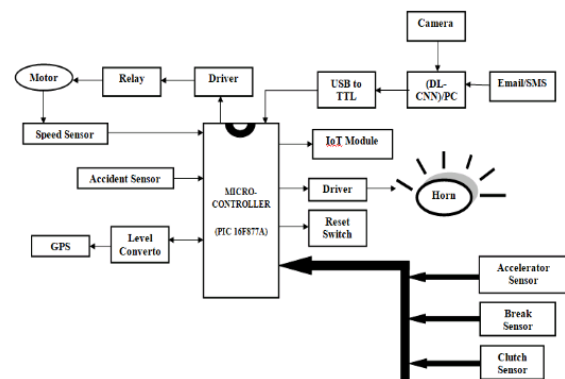
A dataset of images containing roads with lane lines should be collected. The dataset should be augmented by applying various transformations such as rotation, flipping and zooming to increase the amount of training data. The next step is to design the CNN architecture. The proposed model may consist of multiple convolutional and pooling layers, followed by fully connected layers and output layers. The model should be trained on a large dataset using an appropriate loss function and optimizer. The model should be trained on a large dataset using a training algorithm such as Stochastic Gradient Descent (SGT) or Adam Optimizer. During training, the model parameters are updated to minimize the loss function. Finally, the trained model can be used to detect left and right lane lines in real-time. More number of sensors are implemented to identify the activities of vehicles to prevent accident, all the information from sensors will be send to vehicle black box to record the information for future investigation.

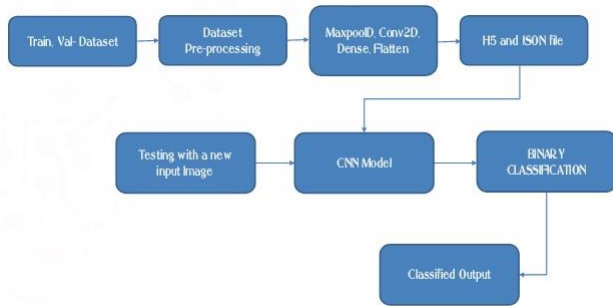
ADVANTAGES

- We can monitor the speed of the vehicle.
- We can find the location of the vehicle.
- Alert message to mobile phone for remote information.
- It is used to vehicle accident evidence and is useful to found victim easily without human intervention
- It is mainly used as a tracking device and we can monitor driver rash driving behavior

V. METHODOLOGY

In this methodology we described about the block diagram, A dataset of images containing roads with lane lines should be collected. The dataset should be augmented by applying various transformations such as rotation, flipping and zooming to increase the amount of training data. The next step is to design the CNN architecture. The model should be trained on a large dataset using a training algorithm such as Stochastic Gradient Descent (SGT) or Adam Optimizer. During training, the model parameters are updated to minimize the loss function. Finally, the trained model can be used to detect left and right lane lines in real-time. More number of sensors are implemented to identify the activities of vehicles to prevent accident, all the information from sensors will be send to vehicle black box to record the information for future investigation. The black box system acquires data from various sensors such as temperature sensor, accident sensor, GPS, accelerator, brake, and clutch. The data acquired from the sensors is processed by the PIC controller, which is responsible for reading the sensor data and converting it into a format that can be used for further analysis. The IoT module and GPS allow the system to transmit real-time data to a remote location for further analysis. This feature helps in keeping track of the vehicle's location and movement. The system is equipped with a reset switch that allows the user to reset the system for minor accident occur.





LIGHT FIELD ROAD LANE DATASET

This paper for the first time presents a light field road lane detection (LFLD) dataset. The benchmark lane detection datasets, such as CULane [47], Tu simple [48], and LLAMAS[49] consist of regular images and therefore, only retain the spatial information of complex real-world scenes. Unlike these standard datasets, LFLD consists of light fields and hence contains the angular information of the light rays in addition to the spatial information. The additional information carries robust features for classification/detection tasks. LFLD dataset consists of 1000 light fields captured across several roads in daylight conditions. It consists of 50 different sequences, each containing 20 light fields captured along a single road section. These sequences are densely sampled, so the dataset can be beneficial for lane detection methods that exploit temporal information (video-based lane detection method) as well as spatial and angular information. One of these sequences is shown in Figure 3, and some randomly selected captures from multiple other sequences are given in Figures 4, 5, 6, and 8. Out of the total 1000 light fields 100 are captured under challenging conditions such as, illumination variations, false lane lines and strong shadows. The remaining 900 light fields are captured under normal conditions. LFLD dataset is captured by the first generation commercially available Lytro [50], light field camera. The captured light fields are decoded to obtain a set of 11 × 11 perspective images, each with the size 375 × 375 pixels, using matlab Light Field Toolbox v0.4 [16], as shown in Figure 2. The dataset has been made public and is available on the link given below.

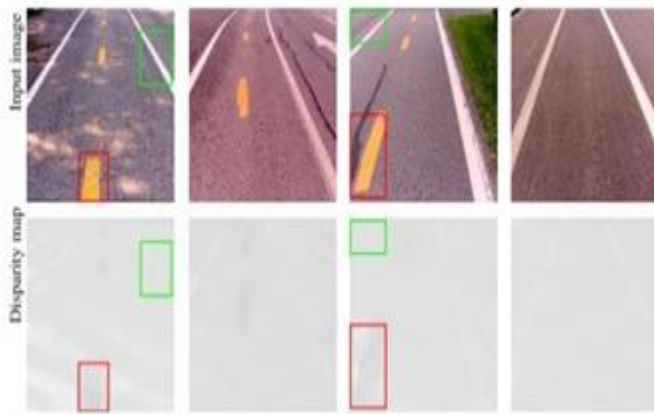
LIGHT FIELD FOR IMPROVED LANE DETECTION

Light field imaging captures the angular information of the light rays originating from a scene point. The MLA based light field cameras, Figure 1(b & c), achieve this by placing an MLA adjacent to the sensor that separately records at different pixels the intensities of light rays passing through different points (sub-apertures) of the main lens and converging at the micro-lens in front of these pixels. However,

in conventional cameras, Figure 1(a), the incident light rays converge directly at the sensor and are recorded, therefore, losing the directional information. Typically, the light rays reflected from scene points at different depths arrive at the MLA with a different angle, Figure 1(b). By tracing light rays back to the scene space, the corresponding depth of these points can be calculated. Depth estimation of all the captured points results in a map that provides the depth variations among different objects in the scene. This depth information is an additional discriminative feature well utilized in classification problems such as face recognition. In case of the road lane detection, depth of the lane lines on the road changes along with the road's depth. Therefore, the scene's depth variation does not provide any valuable information to improve the discrimination between different lane lines and the road. However, color of the lane lines is unique and significantly differs from the road's color as well. Light reflected from the unique color (wavelength) lane line, and the road from the two different points at the same depth passes from the main lens and refracts following the refraction theorem. Therefore, the angle of incidence at MLA of light rays originating from different color points despite the same depth is still different, as shown in Figure 1(c). This variation in incident angle causes disparity in multiple perspective images acquired from the decoded light field. In Figure 4, it can be seen that the disparity changes with the change in color of the lane line. This disparity variation provides an additional discrimination cue that can improve the performance of lane detection methods. It is also worth noticing that despite the change in depth along the road, the disparity seems to be mostly constant. This could be due to the fact that the black road is uniform and there is not enough texture variation on the road for any matching algorithm to



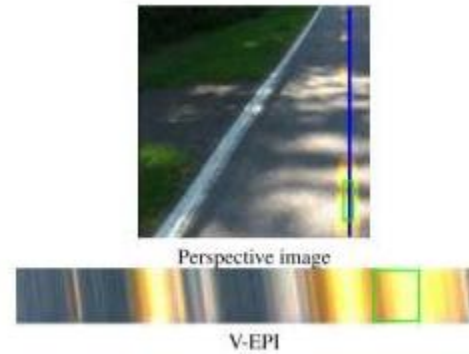
Example sequence of the proposed LFLD dataset.



detect. This significantly improves the effectiveness of the proposed disparity cue, ensuring that disparity variation is only caused by the presence of lane lines on the road. Shades of the road trees and vehicles on the road usually result in occlusion and illumination variation across the lane lines. False lines can also appear on the road, for example shades of high tension wires along the road, as shown in Figure 5. This causes the intensity variation along the lane lines in the captured image and therefore limits their effectiveness in providing sufficient discriminative features for detection. However, the wavelength of the light reflected from a particular color line remains independent of the illumination variation and therefore the angular information remains unaffected. An EPI image can be extracted from a light field by cross-sectioning correspondingly orientated perspectives. For instance, gathering pixels by horizontally cross-sectioning perspectives in horizontal direction results in horizontal EPI. Similarly, vertical EPI can be formed through vertical cross-sectioning of the vertically aligned perspectives. The EPI representation of the light field, the angle of the incident light across a lane line remains



A subset of various challenging conditions for lane detection from our challenging road condition dataset.



An EPI-based illustration of light's incident angle under illumination variations.

unchanged irrespective of the illumination variation. The additional angular information provides robustness against illumination variations and false lines. Multiple viewpoints help significantly in occlusion avoidance, and therefore, the degradation in the overall performance of any lane detection algorithm under these challenging conditions is minimal with the light field as input data.

VI. LIGHT FIELD REPRESENTATION

Light field can be represented in many ways including, perspective images, lens let images, EPIs, and focus stacked images. In this paper, we used light fields in two different forms, a sequence of perspective images and a disparity map estimated through the light field, to take advantage of additional angular information for improved lane detection. Other light field representations, such as Lens let, EPI, and focused stacked image, can be considered by the future lane detection methods that will incorporate LFs as their input.

A. PERSPECTIVE IMAGE REPRESENTATION

Lytro camera's raw light field when decoded with the [16], Matlab's toolbox results in a regular grid of 11 × 11 perspective images which is referred to as its angular resolution and each perspective has a spatial resolution of 375 × 375. We have cropped and resized these perspective images to match CNN's input layer size. In order to exploit the angular information among the perspective images, we used an LSTM layer in our network shown in Figure 7, and detailed below. An LSTM layer is composed of cells and each cell has three inputs, an input feature vector, an input hidden state, and a common cell state. Additionally, each cell has three gates: input, forget, and output gates. Upon the arrival of new information, the network can forget the previous state and update the current state. This structure enables learning long short-term inter-view, angular relationships from the features

extracted through the sequence of perspective images. The overall network architecture includes a convolutional neural network, which is used as a feature extractor and converts a sequence of perspective images into a sequence of feature vectors, where each feature vector is obtained from the last pooling layer of the network independently for each input perspective image and then combined as a sequence. The sequence of feature vectors is fed directly to a sequence input layer with an input size corresponding to the featured dimension of the feature vectors. An input sequence layer is followed by an LSTM layer with 2000 hidden units and a dropout layer afterwards. Finally, a fully connected layer with an output size matching the number of responses and a regression layer are connected.

B. DISPARITY MAP AS INPUT

The variation in the angle of incident light originating from different color lane lines and roads can be represented in the this angular information by directly providing a disparity map as input to the CNN. Since the lane lines are the only color variation on the road data, we assume that using the correct RGB primaries would allow us to represent the color information adequately. For example, only red and green channels can represent a yellow line. However, only in case of the white line, all three color channels are needed and, therefore, the information from one color channel for one lane line is traded for the additional information from disparity for all road lines. In our experiment, we used the Lytro desktop app3to estimate disparity maps. The Lytro app allows the export of gray- scale 16-bit normalized disparity maps from a given LF image. Smoothing is applied to the disparity map by the software with the help of human interaction for noise reduction. Since the entire LF is used in estimating the disparity maps, it is expected to be robust to the matching errors in comparison to the typical stereo systems. We have tested two combinations: discarding a single color channel (blue)of an RGB image and replacing it with the disparity map, and converting an RGB image into gray-scale and replicating the same information in two channels and using the disparity map as the third channel, without changing the input layer touse pre-trained weights. Although this representation results in the information trade-off, it allows us to avoid the extra computation and network modification involved in the LSTM based approach. However, this approach involves an additional pre-processing step of estimating the disparity map. The proposed representation can be used with any existing network for lane detection.

TRAINING

We trained three different CNNs, namely Google Net, VGG-16, and Nasnet. To demonstrate the robustness of the proposed LF representation, we chose these networks which react a wide range of performance variation in terms of prediction accuracy on ImageNet [6] validation dataset. These CNNs are classification networks and for the road lane line points coordinate prediction, we modified them for regression. For GoogleNet, we replaced the `loss3- classi_er`,`prob`,`output` layers with a fully connected (FC) layer with20 responses, to match the coordinate of the lane line points per image and in the end, we added a regression layer. ForVGG-16 we removed the fully connected, `prob`,`output` layers and added an FC and regression layer. For Nasnet, we removed the prediction layers and the classification layer and introduced an additional FC and regression layer. These CNNs are pre-trained on ImageNet dataset and transfer learning is performed to adapt and _ne- tune pre-trained Google Net, VGG-16, and Nasnet for the lane detection problem. For the sequence of perspective images, Pre-trained CNN is used for feature extraction on our road data and LSTM network pre-trained on [51], data is tuned for the lane detection problem. Our road lane dataset, which is captured across different cities, consists of 1000 light _elds, out of which 70 % are used for training the remaining 30% is kept for testing. The simulations show that the network's predictions are robust under different training hyper-parameters configurations. Various combinations of the learning rate, optimizer ,and batch size are tested but the variations in performance are negligible. The batch size turned out to be the most in_ential3http://light_eld-forum.com/lytro/lytro archive/hyper-parameter in terms of performance improvement for both the networks described above. Increasing the batch size improved the performance and the maximum batch size supported due to memory limitations is 32. Among different configurations, the following set of hyperparameters resulted in the best performance and, therefore, adopted in this work. The initial learning rate is set to $3e-4$ with a learning rate drop of 0.1 and a learning rate drop period of 20. Although the choice of optimizer has shown a marginal effect on the overall performance, adam optimizer has slightly improved the prediction and hence selected in our training. The batch size is set to 32 and the training is performed for 40 epochs.

A. EVALUATION METRICS

1) RMSE

Evaluation of the regression model's performance can best be described in terms of error values. For this purpose, we calculated the commonly used root mean square error metric (RMSE) [52] and [53].

where *Predicted* represents the predicted lane line point coordinates value in pixels units, and *Actual* is the ground truth value for the same point coordinates. In practice, Actual and Predicted values are given as two-dimensional vectors with x and y coordinates of the selected points on the lane lines. So the smaller RMSE will indicate that the predicted lane line is closer to the ground truth than a predicted line with a large RMSE.

2) LIOU

We have also used Line IoU loss [42], where possible, for the evaluation of the proposed disparity-based LF representation. Each point in the predicted lane is first extended into a line segment with a radius e . Then IoU, which is the ratio of intersection over union between two line segments, is calculated between the extended line segment and its ground truth.

Where extended points are the corresponding ground truth points. Note that d_i can be negative which can make it feasible to optimize in case of non-overlapping line segments. Then LioU can be considered as the combination of infinite line points. To simplify the expression and make it easy to compute, we transform it into a discrete form, when two lines are far away.

Then the LioU loss is defined as, $LioU=1-LioU$

Where $-1 < LioU < 1$,

When two lines overlay perfectly, then $LioU=1$ converges to -1 when two lines are far away.

3) ACCURACY

Accuracy is another commonly adopted metric for the evaluation of a lane detection model [54], [55]. We applied accuracy for the performance evaluation of the proposed disparity based LF representation using state-of-the-art lane detection methods.

where *Cclip*, *Sclip* are the number of correctly predicted lane line points and the number of ground truth lane line points respectively. A predicted lane is considered correct if more than 85 % of predicted lane line points are within 20 pixels of the corresponding ground truth points.

VII. EXPERIMENTAL RESULTS

This section presents the results of the proposed light field-based lane detection technique. We have evaluated the proposed technique quantitatively and qualitatively by using the evaluation metrics detailed in subsection VI-A, and

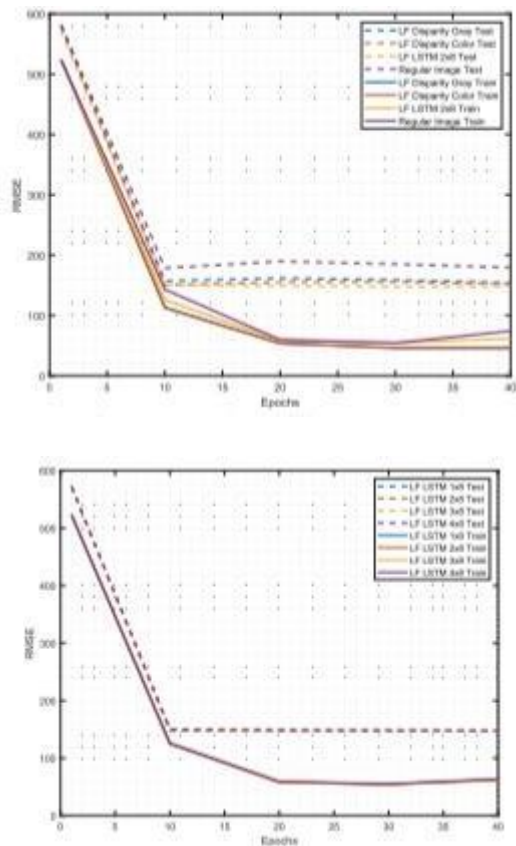
plotting the predicted lane lines compared to the ground truth for visual inspection. We chose only the conventional RGB image to plot for simplification of representation; the lane lines predicted using different light field representations and 2D images against the ground truth.

In Figure 8, it can be seen that in both good and poor quality predictions, the LF-based lane detections are overall closer to the ground truth as compared to the regular image based predictions. However, in this small subset presented in Figure 8, it is unclear that a particular LF representation performs better than the others.

In Figure 9, a quantitative comparison of the different LF representations and regular images (middle perspective image of the decoded LF) is presented. It can be seen in Figure 9, that any LF representation outperforms the regular image-based lane detection by a significant margin. Within different LF representations, a sequence of input perspective images has shown slight improvement over the others. Nevertheless, the sequence-based input requires modification in the network architecture and involves additional computations; however, no additional labeling is required.

The LF perspective image representation, however, does not benefit solely from the increased number of images. The most critical factor is the angular information (Disparity) between these perspectives. In Figure 10, it can be seen that once the angular information between the perspective images is learned by the network, increasing the number of views makes negligible improvement in the performance. We have noticed that up to eight perspective images are sufficient to adequately present the angular information in our case. The impact of viewpoint selection is not considered in this study and will be part of future work along with other possible compact representations. Currently, the horizontal perspective images from the middle row of the decoded light field, Figure 2, are selected. To increase the views points, as presented in Figure 10, the rows on top and underneath the middle row of the decoded light field are added.

The robustness of the proposed light field-based lane detection method in the challenging conditions is evident from Figure 11. In our experiments, the following conditions: illumination variation, shadow, and false lines, highlighted in figure 5, constitute the challenging dataset.



Under these special conditions, the spatial information gets degraded, resulting in performance deterioration of the methods that rely only on the spatial information of the scene. The LF representations provide additional angular information independent of the illumination variations. Multiple view effective in the case of occlusions, and the disparity provides better discrimination against false lines. For the results presented in Figure 11, the network is trained on a regular condition training dataset of 700 images, and only testing is performed on the challenging dataset of 100 samples. It can be seen in Figure 11, that the challenging conditions dataset despite being 13 in size, results in overall higher RMSE as compared to the testing performed on a regular condition dataset presented in Figure 9.

In Table 1, we compare the performance of the LF representations and regular images on two different test data sets. The proposed LF representation (LF Disparity Gray, LF Disparity Color, LF LSTM 2 _ 8) outperforms the regular image data by 14%, 15%, and 18% under normal conditions; however, the difference in performance grows to 20%, 18%, and 26% in challenging conditions. The difference in performance is expected to increase three times given two different conditions have the same number of test samples. In Figure 12, we demonstrate that a CNN model designed for lane detection can benefit primarily from using LFs during training. It can be seen that a network trained on regular

images needs additional 200 images to achieve comparable performance to the network trained using LFs. The difference could be more significant if the network is trained from scratch instead of fine-tuning a pre-trained network. This performance improvement with lesser data can benefit scarce data-set and avoid additional labeling costs.

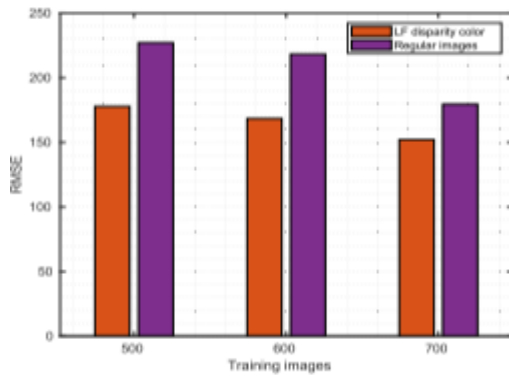
Several deep CNN architectures designed for image classification exist in the literature. Many design choices influence the performance of these CNN models, for example, the number of trainable parameters, Depth, and width of architecture [56]. To demonstrate the robustness of the proposed method across different CNN architectures, which constitute a significant part of most state-of-the-art lane detection methods and is used as a feature extractor in novel learning based methods. We have compared the performance of LF representation with the regular images on two other CNN architecture, namely the VGG-16, and Nasnet presented in Figure 13 and 14.

The performance gap between the VGG-16 and Google Net is marginal; Nasnet, in combination with LSTM trained on the LF data, achieves significant performance improvement. However, for Nasnet, the gap between regular image and disparity-based LF representation reduces only to 6.3 % as Nasnet shows improvement in performance over Google Net and VGG-16 for the regular image dataset. As we used the transfer learning technique to fine-tune the pre-trained models, the networks are biased towards the regular image dataset due to the limited size of LF training data. Since LSTM allows us to maintain the regular RGB image representation and use multiple perspective images to exploit the angular information, it avoids the network's bias. Increasing the data set size for fine-tuning could further increase the performance gap between the disparity-based LF representation and regular image dataset even for complex networks like Nasnet.

Although the three networks are widely different in their design approach, it can be seen that the proposed LF representation in general outperform the regular image based approach. Therefore, the proposed light field-based road lane representation can benefit any existing lane detection method and possibly a new lane detection method such as combining CNN with LSTM or any other network architecture that can exploit the angular information.

In Table 2, we compared the performance of the proposed light field disparity representation with regular images on state-of-the-art methods. The proposed LF representation on lane detection methods explicitly designed for conventional images. It should also be noted that the

backbone networks are pre-trained on Image net [6], which consists of millions of regular images and

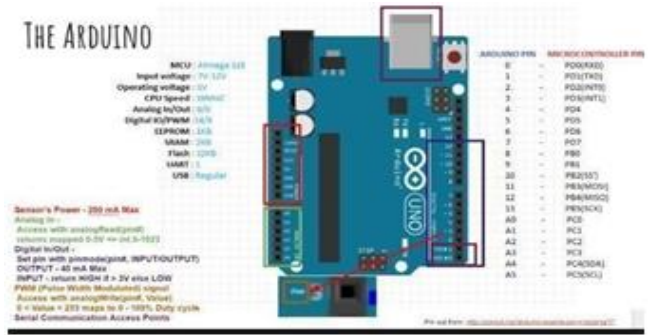


therefore, are biased towards conventional images. The performance gap is expected to increase further with the addition of more training samples in the LFLD dataset during the fine-tuning of the state-of-the-art methods. Additionally, it can be seen in Table 1 and Figure 14, that LF perspective image representation, when used with LSTM, supersedes the LF disparity representation by a significant margin. Therefore, it can be concluded that LF representations not only benefit state-of-the-art lane detection methods but are also worth investigating new methods explicitly designed for exploiting the angular information in addition to spatial information of the scene.

ACCIDENT MONITOR WORKING

When an accident occurred in any place then GPS system tracks the position of the vehicle and sends the information to the particular person through GSM by alerting the person through SMS or by a call.

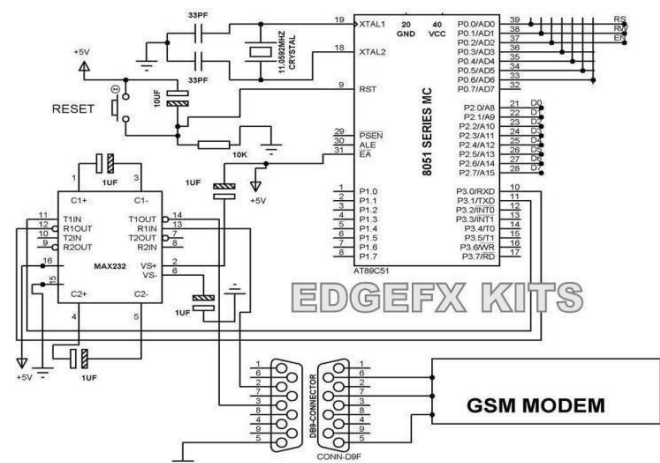
- The Arduino Uno is a microcontroller board based on the ATmega328 (datasheet). It has 14 digital input/output pins (of which 6 can be used as PWM outputs), 6 analog inputs, a 16 MHz ceramic resonator, a USB connection, a power jack, an ICSP header, and a reset button. power it with an AC-to-DC adapter or battery to get started.



POWER: 5V. This pin outputs a regulated 5V from the regulator on the board. The board can be supplied with power either from the DC power jack (7 - 12V), the USB connector (5V), or the VIN pin of the board (7-12V).

Supplying voltage via the 5V or 3.3V pins bypasses the regulator and can damage your board.

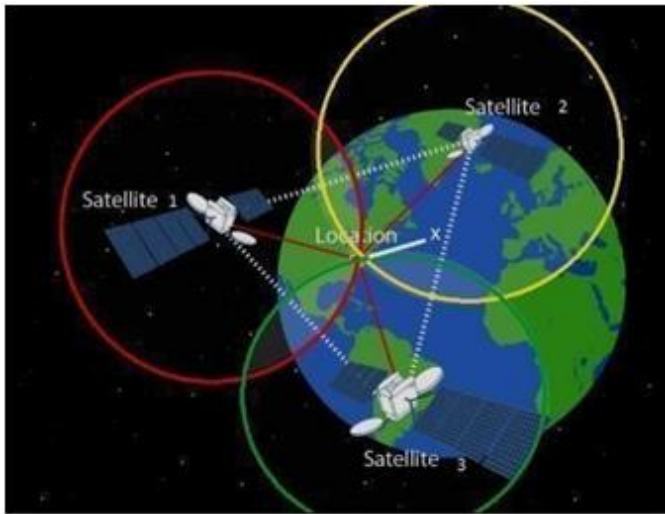
- Vibration sensors are sensors for measuring, displaying, and analysing linear velocity, displacement, proximity, or acceleration. The diagram below is a very simplistic explanation of how vibration data is acquired.
- GSM: From the below circuit, a GSM modem duly interfaced to the MC through the level shifter IC Max232.



- The SIM card mounted GSM modem upon receiving digit command by SMS from any cell phone send that data to the MC through serial communication. While the program is executed, the GSM modem receives the command 'STOP' to develop an output at the MC, the contact point of which is used to disable the ignition switch. The command so sent by the user is based on an intimation received by him through the GSM modem 'ALERT' a programmed message only if the input is

driven low. The complete operation is displayed over a 16x2 LCD display.

- **GPS:** GPS Stands for "Global Positioning system. GPS is a satellite navigation system used to determine the ground position of an object. Each GPS satellite broadcasts a message that includes the satellite's current position, orbit, and exact time. A GPS receiver combines the broadcasts from multiple satellites to calculate its exact position using a process called triangulation. Three satellites are required to determine receiver's location, though a connection to four satellites is ideal since it provides greater accuracy.
- **LCD DISPLAY:** The principle behind the LCD is that when an electrical current is applied to the liquid crystal molecule, tends to untwist.

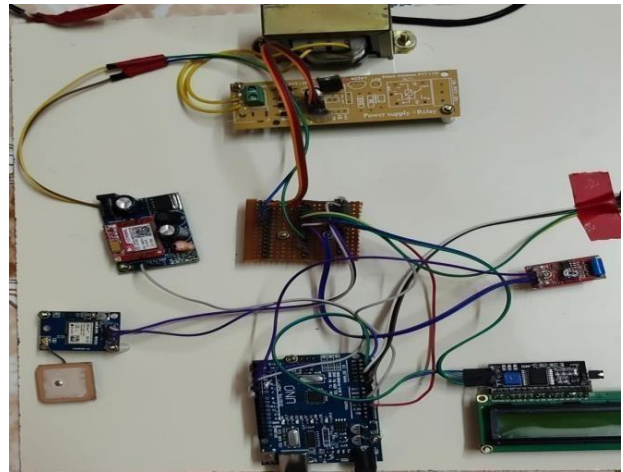


- when an electrical current is applied to the liquid crystal molecule, the molecule tends to untwist. This causes the angle of light which is passing through the molecule of the polarized glass and also causes a change in the angle of the top polarizing filter. As a result, a little light is allowed to pass the polarized glass through a particular area of the LCD. Thus, that particular area will become dark compared to others. The LCD works on the principle of blocking light.

VIII. RESULTS AND DISCUSSION

The below figure shows the hardware implementation of the project where the Arduino is integrated with the components such as accelerometer, vibration sensor, GSM, and GPS modules. In this an accelerometer or vibration sensor is used to detect the accident and then GPS will identify the location and then GSM will establish the network

connection so with the geolocation can be sent to the registered mobile number.



IX. CONCLUSION

The paper presents a LF based lane detection method for improved prediction accuracy. LF representations presented in this paper show significant performance improvement compared to the traditional image-based lane detection approach. The proposed approach improves lane detection by providing additional features that CNNs extract through learning. It can enhance any lane detection method that includes CNN as a feature extractor as well as the non-learning-based approaches with careful consideration towards the hand-crafted features.

REFERENCES

- [1] Y. Ko, Y. Lee, S. Azam, F. Munir, M. Jeon, and W. Pedrycz, "Key points estimation and point instance segmentation approach for lane detection," *IEEE Trans. Intell. Transp. Syst.*, vol. 23, no. 7, pp. 8949-8958, Jul. 2022.
- [2] D. Hopkins and T. Schwanen "Talking about automated vehicles: What do levels of automation do?" *Technol. Soc.*, vol. 64, Feb. 2021, Art. no. 101488.
- [3] H. Abualsaud, S. Liu, D. B. Lu, K. Situ, A. Rangesh, and M. M. Trivedi, "Lane AF: Robust multi-lane detection

- with af_nity_elds," IEEE Robot. Autom. Lett., vol. 6, no. 4, pp. 7477_7484, Oct. 2021.
- [4] S. Yoo, H. S. Lee, H. Myeong, S. Yun, H. Park, J. Cho, and D. H. Kim, "End-to-end lane marker detection via row-wise classification," in Proc. IEEE/CVF Conf. Comput. Vis. Pattern Recognit. Workshops (CVPRW), Jun. 2020, pp. 1006_1007.
- [5] L. Ding, H. Zhang, J. Xiao, C. Shu, and S. Lu, "A lane detection method based on semantic segmentation," Comput. Model. Eng. Sci., vol. 122, no. 3, pp. 1039_1053, 2020.
- [6] H. U. Khan, A. R. Ali, A. Hassan, A. Ali, W. Kazmi, and A. Zaheer, "Lane detection using lane boundary marker network with road geometry constraints," in Proc. IEEE Winter Conf. Appl. Comput. Vis. (WACV), Mar. 2020, pp. 1834_1843.
- [7] Q. Zou, H. Jiang, Q. Dai, and Y. Yue, "Robust lane detection from continuous driving scenes using deep neural networks," IEEE Trans. Veh. Technol., vol. 69, no. 1, pp. 41_54, Mar. 2019.
- [8] W.-J. Yang, Y.-T. Cheng, and P.-C. Chung, "Improved lane detection with multilevel features in branch convolutional neural networks," IEEE Access, vol. 7, pp. 173148_173156, 2019.
- [9] X. Pan, J. Shi, P. Luo, X. Wang, and X. Tang, "Spatial as deep: Spatial CNN for traf_c scene understanding," in Proc. AAAI Conf. Artif. Intell., vol. 32, no. 1, 2018, pp. 7276_7283.
- [10] J. Kim and C. Park, "End-to-end ego lane estimation based on sequential transfer learning for self-driving cars," in Proc. IEEE Conf. Comput. Vis. Pattern Recognit. Workshops (CVPRW), Jul. 2017, pp. 30_38.
- [11] Gowshika, Madhu Mitha, and Jayashree, "Vehicle Accident Detection System By Using GSM And GPS" IRJET, 2019.
- [12] W. Von Rosenberg, T. Chanwimalueang, V. Goverdovsky, D. Looney, D. Sharp, and D. P. Mandic, "Smart Helmet: Wearable Multichannel ECG and Ee G," IEEE J. Transl. Eng. Heal. Med., vol. 4, no. August, pp. 1- 11, 2016.
- [13] X. Pan, J. Shi, P. Luo, X. Wang, and X. Tang, "Spatial as deep: Spatial CNN for traf_c scene understanding," in Proc. AAAI Conf. Artif. Intell., vol. 32, no. 1, 2018, pp. 7276_7283.
- [14] W.-J. Yang, Y.-T. Cheng, and P.-C. Chung, "Improved lane detection with multilevel features in branch convolutional neural networks," IEEE Access, vol. 7, pp. 173148_173156, 2019.
- [15] J. Kim and C. Park, "End-to-end ego lane estimation based on sequential transfer learning for self-driving cars," in Proc. IEEE Conf. Comput. Vis. Pattern Recognit. Workshops (CVPRW), Jul. 2017, pp. 30_38.